nature geoscience

LETTERS

PUBLISHED ONLINE: XX MONTH XXXX | DOI: 10.1038/NGEO2182

Indonesian vegetation response to changes in rainfall seasonality over the past 25,000 years

Nathalie Dubois[1†*], Delia W. Oppo[1*], Valier V. Galy[2], Mahyar Mohtadi[3], Sander van der Kaars[4,5], Jessica E. Tierney[1], Yair Rosenthal[6,7], Timothy I. Eglinton[8], Andreas Lückge[9] and Braddock K. Linsley[10]

The hydrologic response to climate forcing in the Indo-Pacific warm pool region has varied spatially over the past 25,000 years[1-5]. For example, drier conditions are inferred on Java and Borneo for the period following the end of the Last Glacial Maximum, whereas wetter conditions are reconstructed for northwest Australia[4]. The response of vegetation to these past rainfall variations is poorly constrained. Using a suite of 30 surface marine sediment samples from throughout the Indo-Pacific warm pool, we demonstrate that today the stable isotopic composition of vascular plant fatty acids (δ^{13}CFA) reflects the regional vegetation composition. This in turn is controlled by the seasonality of rainfall consistent with dry season water stress[6]. Applying this proxy in a sediment core from offshore northeast Borneo, we show broadly similar vegetation cover during the Last Glacial Maximum and the Holocene, suggesting that, despite broadly drier glacial conditions[1,7], there was no pronounced dry season. In contrast, δ^{13}CFA and pollen data from a core off the coast of Sumba indicate an expansion of C_4 herbs during the most recent glaciation , implying enhanced aridity and water stress during the dry season. Holocene vegetation trends are also consistent with a response to dry season water stress. We therefore conclude that vegetation in tropical monsoon regions is susceptible to increases in water stress arising from an enhanced seasonality of rainfall, as has occurred[8] in past decades.

Indonesia lies at the heart of the Indo-Pacific Warm Pool (IPWP)—the largest reservoir of warm water on Earth. The IPWP sustains deep atmospheric convection and heavy rainfall across the region. On seasonal timescales, the migration of the Intertropical Convergence Zone (ITCZ) and monsoon coupled systems determines the distribution of rainfall (Supplementary Fig. 1 and Supplementary Information 1). Whereas Borneo experiences sustained year-round precipitation, rainfall seasonality increases southward and northward of the island (Fig. 1). On longer (10^3–10^4 yr) timescales, changes in insolation, sea level, the intensity of the Atlantic Meridional Overturning Circulation (AMOC), and land–sea, zonal and meridional temperature gradients influence IPWP rainfall[1,2,7,9,10]. Here, we explore the influences of changes in seasonal rainfall variations during the past 25,000 years on regional vegetation.

Modern vegetation is not uniform throughout our study area. Tropical lowland and montane rainforests dominate on Borneo, Sulawesi and the Moluccas[11]. On the Lesser Sunda Islands, monsoon forests dominate and evergreen rainforests are restricted to isolated patches and mountain sites[11]. In northern Australia, the vegetation consists mainly of eucalyptus open forests and woodlands, with extensive grasslands and small mangrove communities within river estuaries[12].

Whereas global coupled models generally agree that the region was colder and drier during the Last Glacial Maximum (LGM, 23–19 kyr BP; BP = before present) owing to the exposed Sunda Shelf[7], the response of vegetation to these climate changes is not well known. A dynamic vegetation model simulation, for example, suggests that tropical forests dominated the landscape, even over much of the exposed Sunda Shelf[13]. Direct evidence suggests tropical rainforest at some sites and herb expansion in others[14,15], but the reasons for these differences are not understood.

We evaluate the response of terrestrial vegetation to regional hydroclimate variability using the carbon stable isotopic composition (reported as δ^{13}C) of the C_{30} *n*-alkanoic fatty acid (δ^{13}CFA) preserved in sediments from the Indonesian Seas (Supplementary Figs 2 and 3 and Supplementary Information 2 and 3). Long-chain, even-carbon-numbered saturated FA (C_{28}–C_{34}) are synthesized nearly exclusively by vascular plants as components of epicuticular leaf waxes[16]. Rivers and wind carry plant waxes to lakes and the ocean, where they can be stored in sediments, providing records of the past vegetation distribution in nearby catchments[17]. The δ^{13}CFA in sediments thus reflects the distribution of plants over land, mainly the ratio between C3 (δ^{13}CFA = −30.8‰ to −41.8‰) and C4 (δ^{13}CFA = −19.3‰ to −21.6‰) plants[18–20]. The C4 photosynthetic pathway is used by plants (mostly grasses) in tropical environments to limit water loss and results in less isotopic fractionation (higher δ^{13}C values) than the C3 pathway[21].

To assess how well δ^{13}CFA reflects regional vegetation composition, we measured δ^{13}CFA in surface marine sediments ($n = 30$) spanning 35° of longitude and 20° of latitude within the IPWP region (Supplementary Table 1). We find that δ^{13}CFA values increase with southern latitude, indicating an increasing contribution of C4 plants (Fig. 2). The correlation of surface sediment δ^{13}CFA values to the coefficient of variation of rainfall over nearby land (CV, computed as the ratio of the standard deviation of

[1]Department of Geology and Geophysics, Woods Hole Oceanographic Institution, Woods Hole, Massachusetts 02543, USA, [2]Department of Marine Chemistry and Geochemistry, Woods Hole Oceanographic Institution, Woods Hole, Massachusetts 02543, USA, [3]MARUM–Center for Marine Environmental Sciences, University of Bremen, Bremen, Germany, [4]Centre for Palynology and Paleoecology, Department of Geography and Environmental Science, Monash University, Clayton, VIC 3800, Australia, [5]Cluster Earth & Climate, Department of Earth Sciences, Faculty of Earth and Life Sciences, Vrije Universiteit, De Boelelaan 1085, 1081 HV Amsterdam, The Netherlands, [6]Institute of Marine and Coastal Sciences, Rutgers, The State University, New Brunswick, New Jersey 08901, USA, [7]Department of Geology, Rutgers, The State University, New Brunswick, New Jersey 08901, USA, [8]ETH Zurich, Zurich, Switzerland, [9]Bundesanstalt für Geowissenschaften und Rohstoffe (BGR), 30655 Hannover, Germany, [10]Lamont-Doherty Earth Observatory of Columbia University, Palisades New York 10694, USA. †Present address Eawag, Dübendorf, Switzerland *e-mail: nathalie.dubois@eawag.ch; doppo@whoi.edu

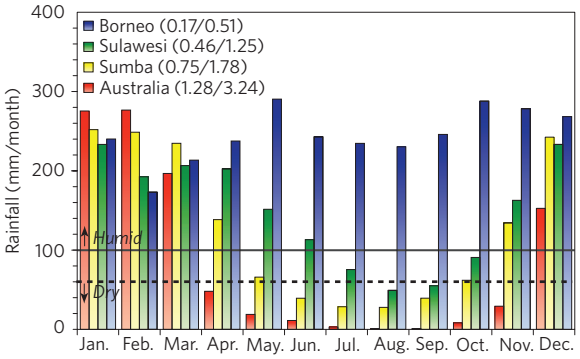

Figure 1 | Histograms of mean monthly rainfall averaged over 1979–2010 (ref. 26). From north to south: Palawan (117.5–120° E, 7.5–10° N), Borneo (115–117.5° E, 2.5–5° N), Sulawesi (117.5–120° E, 2.5–5° S), Sumba (120–122.5° E, 7.5–10° S), and northwest Australia (122.5–125° E, 16.25° S). Numbers in brackets correspond to the coefficient of rainfall variability (CV) and seasonality, respectively (Methods). Horizontal lines indicate humid season (above the solid line, >100 mm) and dry seasons[27] (below the dashed line, <60 mm). White squares in Fig. 2 indicate the locations of the grid points used for rainfall data

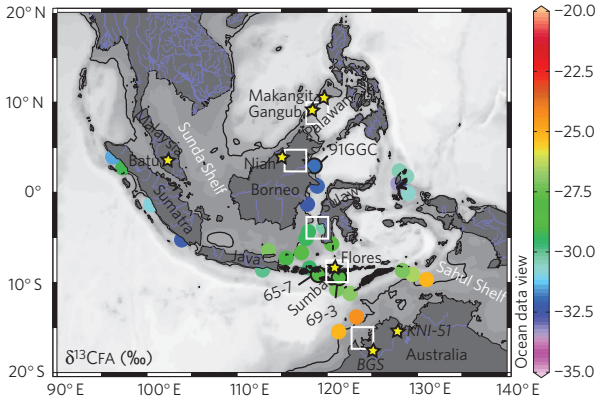

Figure 2 | Map of the δ^{13}C value of the C_{30} *n*-alkanoic fatty acid (δ^{13} CFA) distribution in surface sediments from the IPWP. Yellow stars represent cave locations on Palawan, Borneo, Peninsular Malaysia, Flores and northwest Australia. Gravity cores analysed for palaeoclimatic reconstruction are identified by black circles: BJ8-03-91GGC (91GGC; 2° 52.434′ N, 118° 23.133′ E, 2326m wd), GeoB10069-3 (69-3; 9° 35.69′ S, 120° 55.02′ E, 1250 m), and GeoB10065-7 (65-7; 9° 13.42′ S, 118° 53.61′ E, 1292 m). White squares indicate the location of the grid points used for rainfall data in Fig. 1. Solid black line indicates the 100 m isobaths. The Lesser Sunda Islands are shown in a darker grey. Figure constructed in Ocean Data View[28].

climatological monthly rainfall to the mean monthly precipitation) is much higher than its correlation to mean monthly rainfall (Fig. 3), suggesting that the relative variability of precipitation throughout the year, or rainfall seasonality, and especially its effect on dry season water stress largely controls vegetation composition in the IPWP (Methods, Supplementary Fig. 5 and Supplementary Information 4). The strong correlation suggests that other potential influences, such as a bias towards the delivery of gallery forest (C3) vegetation with greater size of the catchment basin, are minor relative to the strong control of dry season water stress.

We use δ^{13}CFA in marine cores from offshore northern (BJ8-03-91GGC; hereafter 91GGC) and southern Indonesia (GeoB10069-3; hereafter 69-3, and core GeoB10065-7 hereafter 65-7) to infer past variations in vegetation. Radiocarbon dates of planktonic foraminifera provide age models for these records (Supplementary Table 2, Supplementary Fig. 6 and Supplementary Information 5). δ^{13}CFA values increase from −33‰ during the LGM to −31‰ during the Holocene. Even though most of this increase is accomplished in two abrupt steps, δ^{13}CFA values indicate a persistent predominance of C3 vegetation on northeast Borneo (91GGC) during both the LGM and Holocene (Fig. 4), consistent with results from the δ^{13}C of insect cuticles preserved in cave guano profiles (ref. 14; Supplementary Fig. 7). By contrast the δ^{13}CFA record from offshore Sumba (69-3) reveals a shift from a maximum of about −25‰ at the end of the LGM to a minimum of about −29‰ in the mid-Holocene (Fig. 4), with superimposed millennial events. New palynological data from core 69-3 confirm that δ^{13}CFA variations reflect vegetation changes (Fig. 4 and Supplementary Fig. 8).

The δ^{13}CFA values and pollen data suggest that C4 grasslands made up more of the landscape on Sumba during the LGM (Fig. 4). Both charcoal abundance and the number of dry months, as estimated from pollen transfer functions, suggest that prolonged droughts were most common during the LGM, consistent with ~~pollen and~~ δ^{13}CFA evidence for greatest water stress (Fig. 4, Supplementary Information 6 and Supplementary Fig. 8). Measurements of δ^{13}C in cave guano profiles indicate greater C4 vegetation on Palawan, northwest of Borneo and on the Malay Peninsula during the LGM (ref. 14) (Fig. 2 and Supplementary Fig. 9), as we also infer at Sumba.

The dominance of C4 vegetation (grasslands) during the LGM on Sumba suggests an increase in the intensity and duration of the dry season (Jun.–Sept.; Fig. 1). Exposure of the Sahul Shelf may have also reduced moisture flux from the Pacific during the austral fall and winter, reinforcing the influence of the Sunda Shelf (Fig. 1). A longer or more severe dry season on Palawan (currently Feb.–Apr.; Fig. 1) may explain the greater contribution of C4 vegetation (Supplementary Fig. 9) as on Sumba. Thus, in monsoonal regions of Indonesia, LGM drying increased dry season water stress. Evidence of greater C4 vegetation on Peninsular Malaysia[14] suggests the presence of a dry season during the LGM, possibly boreal winter (ref. 7). Although LGM aridity over Borneo—then part of the exposed Sunda Shelf—may have been as great as in the monsoonal regions and the Malay Peninsula, it was not sufficient in any season to result in a pronounced dry season and significantly alter the vegetation.

Following the LGM and coincident with Heinrich Stadial 1 (HS1, ~18–14.7 kyr BP), a North Atlantic cold event[22], δ^{13}CFA values and C4 herb pollen abundance decreased (Fig. 4). Slightly opposite conditions occurred briefly coincident with the Bølling-Allerød (BA), a European/North Atlantic warm period[22]. After the BA event, δ^{13}CFA and pollen data indicate a trend of increasing C3 vegetation, culminating between ~7 and 5.5 kyr ago, followed by a trend reversal towards greater C4 vegetation in the late Holocene. An abrupt increase in C4 vegetation at ~2 kyr ago is superimposed on this trend. These mid-late Holocene features are replicated in core 65-7, and are similar to vegetation changes in northwestern Australia[23].

The deglacial and Holocene δ^{13}CFA and pollen variations observed at our southern sites, although not as well resolved, bear some resemblance to δ^{18}O trends in northern Australian speleothems (Fig. 4), where relatively low values before the LGM, during HS1, and the mid-Holocene are inferred to indicate a stronger austral summer monsoon[3,4]. Hydrologic[1–4] and vegetation (Fig. 4) variability associated with HS1 were probably mediated by variations in the AMOC and accompanying changes in the interhemispheric temperature gradient[10]. However, our data add to a growing body of evidence that HS1 had a greater influence on the IPWP hydrologic cycle than the Younger Dryas (YD, ~12.9–11.7 kyr BP; refs 1,4), another North Atlantic cold event, that is not well defined at Sumba or in Australian speleothems (Fig. 4).

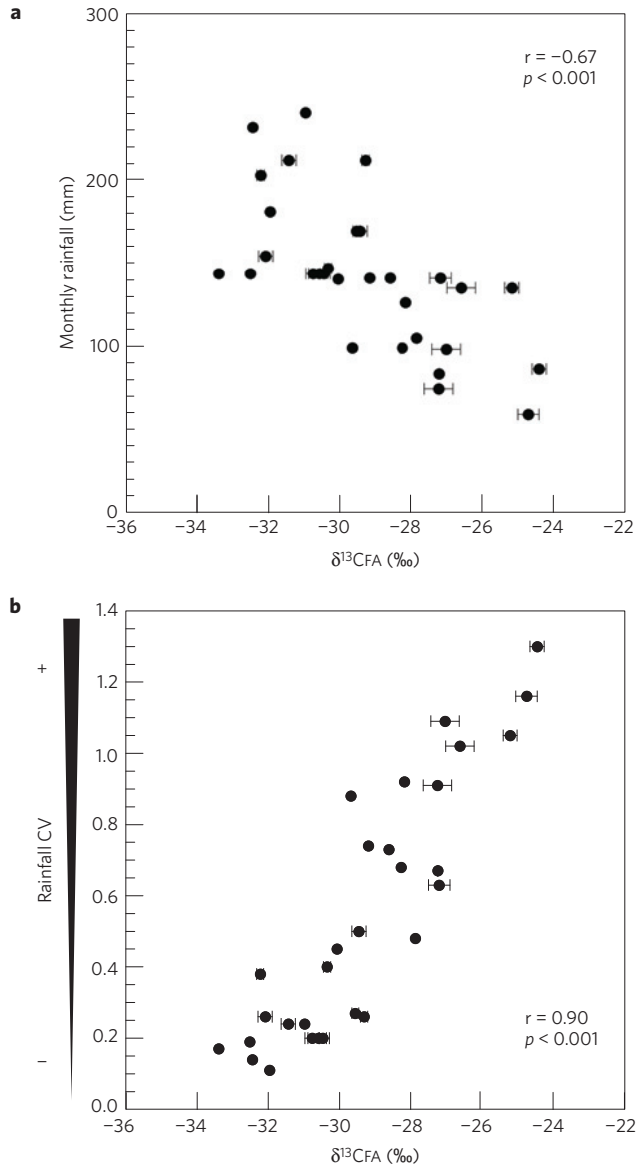

Figure 3 | Coretop δ^{13} CFA versus precipitation data on nearby land[26]. **a**, δ^{13}CFA versus mean monthly precipitation[26]. **b**, δ^{13}CFA versus the rainfall coefficient of variation (CV). Error bars represent standard deviation of replicate measurements.

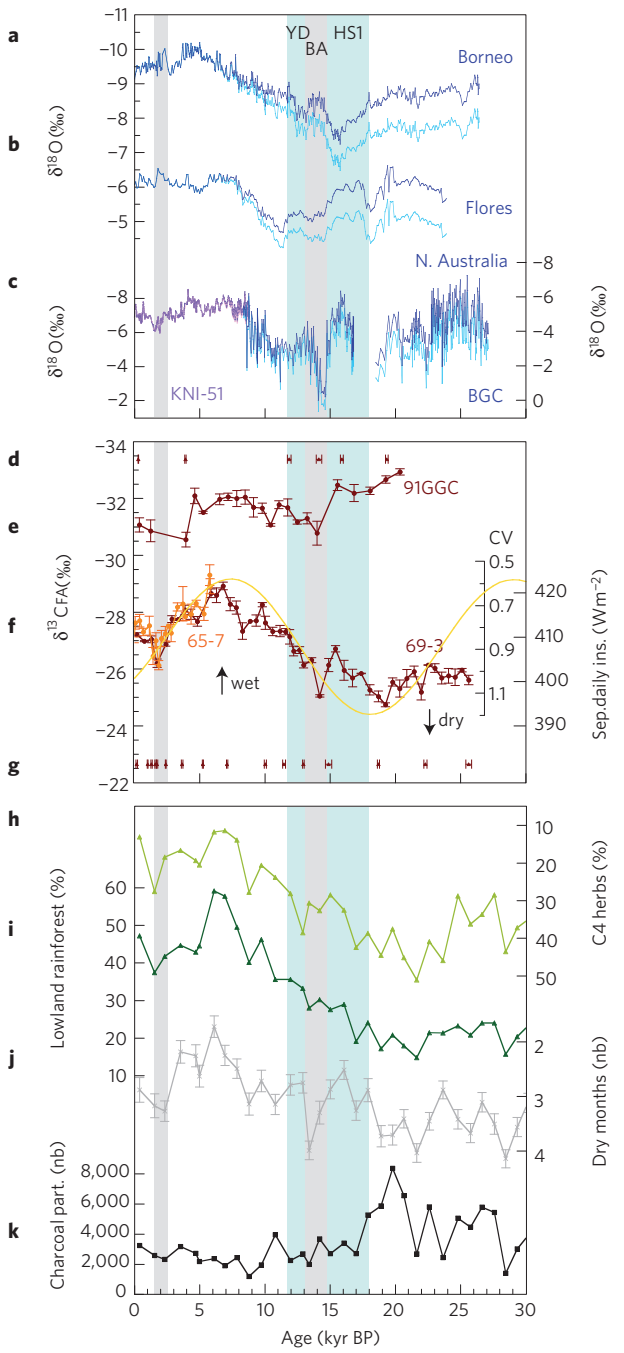

Figure 4 | Downcore δ^{13} CFA compared to pollen data from core 69-3 and IPWP speleothem δ^{18}O records. **a**, Borneo speleothem δ^{18}O record[1]. **b**, Spliced composite Flores speleothem δ^{18}O record[29]. **c**, NW Australia speleothem δ^{18}O records[3,4]. Note that visual overlap between records from the two sites, which have different mean δ^{18}O values, was accomplished by placing them on separate *y*-axes. **d**, AMS-^{14}C age control points for 91GGC. **e**, δ^{13}CFA from 91GGC. **f**, δ^{13}CFA from 69-3 (brown) and 65-7 (orange) along with September daily insolation at 10° S. **g**, AMS-^{14}C age control points for 69-3. **h**, C4 herbs pollen counts in 69-3. **i**, Lowland rainforest pollen counts in 69-3. **j**, Number of dry months based on the pollen transfer function in 69-3. Error bars represent standard error. **k**, Charcoal particles abundance in 69-3. Vertical blue shading indicates the Younger Dryas (YD) and Heinrich Stadial 1 (HS1) and grey shading indicates the Bølling-Allerød (BA) and the 2 kyr event. Darker colours in **a**–**c** show δ^{18}O speleothem data corrected for the ice volume-related changes in sea water δ^{18}O during the last glacial stage[30]. Error bars in **e** and **f** represent standard deviation of replicate measurements.

In the IPWP, insolation-forced ITCZ migration alone cannot explain spatial and temporal trends indicated by Holocene proxy records[3,5]. Holocene trends in hydroclimate of the region are largely driven by the complex interplay between insolation and ocean–atmosphere interactions[5,23]. For instance, upwelling records from offshore S. Java reflect the strength of cross-equatorial southeasterly winds, which are strongest in boreal summer[24]. In contrast, the vegetation records presented here reflect water stress during the dry season, which occurs later in the year. On the basis of our evidence that greater dry season rainfall reduces water stress, we infer higher rainfall over Sumba late in the dry season (September; Figs 1 and 4) from ~5–7 kyr, when δ^{13}CFA reach minimum values (Fig. 4). An increase in precipitation at the end of the dry season may be a response to direct insolation forcing, as is hypothesized on Borneo[1], or alternatively may be due to a lagged insolation response between the Indian Monsoon and Indian Walker Circulation[5]. Both of these mechanisms would have reduced water stress at Sumba (and Palawan and the Malay Peninsula) in the mid-Holocene.

Holocene vegetation trends at Sumba more closely parallel δ^{18}O trends in northern Australia than in Flores speleothems (Fig. 4), despite the closer proximity of Flores to Sumba; notably the mid-late Holocene trend of inferred increasing dry season aridity that culminates in an event at ~2 kyr. This trend, although not as pronounced, is seen in northern Australia but not at Flores. The abrupt vegetation change at ~2 kyr ago corresponds to proportionally more C4 vegetation and increased rainfall seasonality, which is also recorded in northwestern Australia[3,23]. This 2 kyr event is coincident with an inferred weaker austral summer monsoon in northern Australia and an inferred stronger austral summer monsoon at Flores, Borneo (Fig. 4) and Java[24]. The difference between our records from Sumba and the Flores speleothem suggests an opposite hydrologic response between the two sites, possibly related to elevation differences. Discrepancies between the Flores speleothem and Sumba δ^{13}CFA records may also be a function of the different climate signals preserved in the proxies: the δ^{13}CFA primarily records variations in dry season water stress, but the δ^{18}O speleothem records from Flores may primarily reflect wet season moisture variability[2]. However, we cannot rule out further controls on the speleothem δ^{18}O in this region. For example, in addition to the effects of rainfall amount and seasonality on speleothem δ^{18}O, the source and isotopic composition of the rainfall may change, and temperature changes may influence the speleothem δ^{18}O (ref. 25), although in this region the effect of temperature is probably negligible on this timescale. Palaeoclimate archives indicate significant zonal and meridional reorganization of Indo-Pacific precipitation at this time[3,9], with regional heterogeneity, but further research is needed to understand the cause of these late Holocene features.

Our study demonstrates the strong sensitivity of vegetation to both gradual and abrupt changes in rainfall regimes in southern Indonesia. Although changes in rainfall seasonality documented during the past 25 kyr were probably larger than those occurring today—and resulting from different causes—our results underscore the likelihood that natural vegetation will change in response to the trend of increasing seasonality in monsoon regions of the IPWP and other tropical monsoon regions where seasonality and rainfall abundance are changing[8]. In these regions, millions of lives depend on the regularity of seasonal rainfall for agriculture.

Methods

The coefficient of rainfall variability (CV) was computed as the ratio of the standard deviation of climatological monthly (January–December) rainfall[26] (1979–2010) to the mean monthly precipitation (climatological annual mean rainfall divided by 12). The simple seasonality index was computed by subtracting the average rainfall during the driest month from the average rainfall in the wettest month, and dividing this difference by the mean monthly rainfall. The Pearson correlation coefficient between these two indices is 0.99 ($p < 0.001$; Supplementary Fig. 5a).

5–10 g of sediments were freeze-dried and homogenized before lipid extraction using a microwave-assisted reaction system (MARS). Fatty acids were isolated from the total lipid extract by aminopropyl-silica-gel column chromatography, methylated with methanol of known isotopic composition, and then further purified by aminopropyl-silica-gel chromatography and silver nitrate-silica-gel chromatography. Fatty acid methyl esters were analysed in triplicate for their carbon isotopic composition by means of gas chromatography-isotope ratio monitoring-mass spectrometry (GC-IR-MS) at the Woods Hole Oceanographic Institution. All δ^{13}C values were normalized to the VPDB scale using multiple pulses of CO_2 reference gas. The average standard deviation of replicate measurements was 0.19‰. Measurements were corrected for the added methyl group on the basis of isotopic mass balance.

For palynological processing 5.3–7.5 ml of sediment were suspended in approximately 40 ml of tetra-sodium-pyrophosphate (±10%), sieved over 200 and 7 micrometre screens. Following hydrochloric acid (10%) treatment, heavy liquid separation (sodium-polytungstate, SG 2.0, 20 min at 2,000 rpm, twice), acetolyis and sodium carbonate (20%) treatment, the resulting organic residues were mounted in glycerol and slides sealed with paraffin wax. Palynological slides were counted along evenly spaced transects until a minimum count of 100 dryland rainforest pollen grains was reached. All percentage values presented here are based on the total dryland pollen sum made up of all terrestrial pollen grains counted (that is, excluding mangrove pollen and pteridophyta spores). This pollen sum varied between 322 and 964, with an average of 527 pollen grains. Pollen taxa were placed into ecological groups according to where they most commonly occur. See Supplementary Information 6 and Supplementary Fig. 6 for details of the transfer function calculation.

Received 20 February 2014; accepted 7 May 2014; published online XX Month XXXX

References

1. Partin, J. W., Cobb, K. M., Adkins, J. F., Clark, B. & Fernandez, D. P. Millennial-scale trends in west Pacific warm pool hydrology since the Last Glacial Maximum. *Nature* **449,** 452–455 (2007).
2. Griffiths, M. L. *et al.* Increasing Australian–Indonesian monsoon rainfall linked to early Holocene sea-level rise. *Nature Geosci.* **2,** 636–639 (2009).
3. Denniston, R. F. *et al.* A Stalagmite record of Holocene Indonesian Australian summer monsoon variability from the Australian tropics. *Quaternary Sci. Rev.* **78,** 155–168 (2013).
4. Denniston, R. F. *et al.* North Atlantic forcing of millennial-scale Indo-Australian monsoon dynamics during the Last Glacial period. *Quaternary Sci. Rev.* **72,** 159–168 (2013).
5. Tierney, J. E. *et al.* The influence of Indian Ocean atmospheric circulation on Warm Pool hydroclimate during the Holocene epoch. *J. Geophys. Res.* **117,** D19108 (2012).
6. O'Leary, M. H. Carbon isotope fractionation in plants. *Phytochemistry* **20,** 553–568 (1981).
7. DiNezio, P. N. & Tierney, J. E. The effect of sea level on glacial Indo-Pacific climate. *Nature Geosci.* **6,** 485–491 (2013).
8. Feng, X., Porporato, A. & Rodriguez-Iturbe, I. Changes in rainfall seasonality in the tropics. *Nature Clim. Change* **3,** 811–815 (2013).
9. Tierney, J. E., Oppo, D. W., Rosenthal, Y., Russell, J. M. & Linsley, B. K. Coordinated hydrological regimes in the Indo-Pacific region during the past two millennia. *Paleoceanography* **25,** PA1102 (2010).
10. Gibbons, F. T. *et al.* Deglacial δ^{18}O and hydrologic variability in the tropical Pacific and Indian Ocean. *Earth Planet. Sci. Lett.* **387,** 240–251 (2014).
11. Collins, N. M., Sayer, J. A. & Whitmore, T. C. *The Conservation Atlas of Tropical Forests: Asia and the Pacific* (Macmillan Press, London 1991).
12. Beadle, N. C. W. *The vegetation of Australia* (Cambridge Univ. Press, 1981).
13. Prentice, I. C., Harrison, S. P. & Bartlein, P. J. Global vegetation and terrestrial carbon cycle changes after the last ice age. *New Phytologist* **189,** 988–998 (2011).
14. Wurster, C. M. *et al.* Forest contraction in north equatorial Southeast Asia during the Last Glacial Period. *Proc. Natl Acad. Sci.* **107,** 15508–15511 (2010).
15. Sun, X. J., Luo, Y. L., Huang, F., Tian, J. & Wang, P. X. Deep-sea pollen from the South China Sea: Pleistocene indicators of East Asian monsoon. *Mar. Geol.* **201,** 97–118 (2003).
16. Eglinton, G. & Hamilton, R. J. Leaf Epicuticular Waxes. *Science* **156,** 1322–1335 (1967).
17. Rieley, G. *et al.* Sources of sedimentary lipids deduced from stable carbon-isotope analyses of individual compounds. *Nature* **352,** 425–427 (1991).
18. Fang, J., Kawamura, K., Ishimura, Y. & Matsumoto, K. Carbon isotopic composition of fatty acids in the Marine Aerosols from the Western North Pacific: Implication for the source and atmospheric transport. *Environ. Sci. Technol.* **36,** 2598–2604 (2002).
19. Chikaraishi, Y., Naraoka, H. & Poulson, S. R. Hydrogen and carbon isotopic fractionations of lipid biosynthesis among terrestrial (C3, C4 and CAM) and aquatic plants. *Phytochemistry* **65,** 1369–1381 (2004).
20. Matsumoto, K., Kawamura, K., Uchida, M. & Shibata, Y. Radiocarbon content and stable carbon isotopic ratios of individual fatty acids in subsurface soil: Implication for selective microbial degradation and modification of soil organic matter. *Geochemic. J.* **41,** 483–492 (2007).
21. Deines, P. in *Handbook of Environmental Isotope Geochemistry* (eds Fritz, P. & Fontes, J. C.) 329–406 (Elsevier, 1980) Flexor, J. M. and Volkoff, B.
22. Alley, R. B. & Clark, P. U. The deglaciation of the northern hemisphere: A global perspective. *Ann. Rev. Earth Planet. Sci.* **27,** 149–182 (1999).
23. McGowan, H., Marx, S., Moss, P. & Hammond, A. Evidence of ENSO mega-drought triggered collapse of prehistory aboriginal society in northwest Australia. *Geophy. Res. Lett.* **39,** L22702 (2012).
24. Mohtadi, M. *et al.* Glacial to Holocene swings of the Australian–Indonesian monsoon. *Nature Geosci.* **4,** 540–544 (2011).
25. Griffiths, M. L. *et al.* Younger Dryas–Holocene temperature and rainfall history of southern Indonesia from δ^{18}O in speleothem calcite and fluid inclusions. *Earth and Planet. Sci. Lett.* **295,** 30–36 (2010).

26. Adler, R. F. *et al.* The Version-2 Global Precipitation Climatology Project (GPCP) monthly precipitation analysis (1979–Present). *J. Hydrometeor.* **4,** 1147–1167 (2003).
Q.5 27. Schmidt, F. H. & Ferguson, J. H. A. Rainfall types based on wet and dry period ratios for Indonesia with western New Guinea. *verhandelingen djawatan meteorologi dan geofisika djakarta* **42,** 77 (1951).
Q.6 28. Schlitzer, R. Ocean Data View, http://odv.awi.de (2012).
29. Ayliffe, L. K. *et al.* Rapid interhemispheric climate links via the Australasian monsoon during the last deglaciation. *Nature Commun.* **4,** 2908 (2013).
30. Mitrovica, J. X., Gomez, N. & Clark, P. U. The sea-level fingerprint of west Antarctic collapse. *Science* **323,** 753 (2009).

Acknowledgements

This research was supported by NSF grants ABR-86074300 and OCE-1333387, and BMBF grant PABESIA. X. Philippon, C. Johnson, S. Sylva, D. Montluçon, K. A. Rose and A. Gorin provided invaluable technical assistance. W. Kuhnt generously shared Timor Sea core-top samples from cruise SO-185.

Author contributions

D.W.O. designed the study with input from all co-authors. ND generated the δ^{13}CFA data, with guidance from V.V.G., J.E.T. and T.I.E.. S.v.d.K. generated the pollen data. N.D. and D.W.O. wrote the paper with input from all co-authors.

Additional information

Supplementary information is available in the online version of the paper. Reprints and permissions information is available online at www.nature.com/reprints. Correspondence and requests for materials should be addressed to N.D. or D.W.O.

Competing financial interests

The authors declare no competing financial interests.

Queries for NPG paper ngeo2182

Page 1

Query 1:
Please provide post code for 3rd and 8th affiliation.

Page 2

Query 2:
Figure 1 caption mentions five locations including Palawan. The figure itself shows no data for Palawan (Palawan does appear on Fig. 2).

Query 3:
Please note that reference numbers are formatted according to style in the text, so that any reference numbers following a symbol or acronym are given as 'ref. XX' on the line, whereas all other reference numbers are given as superscripts.

Page 4

Query 4:
Please define VPDB.

Page 5

Query 5:
Please check journal title and page range for ref 27.

Query 6:
Is ref 28 a simple website reference (latest update is March 31 2014) in which case no author is necessary or does the author named imply a particular page on the website.